Comp. Appl. Math. (2018) 37:2519–2532
https://doi.org/10.1007/s40314-017-0461-x

CrossMark

A line search algorithm for wind field adjustment with incomplete data and RBF approximation

Daniel A. Cervantes[1] · **Pedro González Casanova**[1] · **Christian Gout**[2] · **Miguel Ángel Moreles**[3]

Received: 20 December 2016 / Revised: 2 May 2017 / Accepted: 28 May 2017 / Published online: 12 June 2017

Abstract The problem of concern in this work is the construction of free divergence fields given scattered horizontal components. As customary, the problem is formulated as a PDE constrained least squares problem. The novelty of our approach is to construct the so-called adjusted field, as the unique solution along an appropriately chosen descent direction. The latter is obtained by the adjoint equation technique. It is shown that the classical adjusted field of Sasaki's is a particular case. On choosing descent directions, the underlying mass consistent model leads to the solution of an elliptic problem which is solved by means of a radial basis functions method. Finally, some numerical results for wind field adjustment are presented.

Keywords Wind adjustment · RBF methods · Line search

Mathematics Subject Classification 65K10 · 65N35 · 35Q86

Communicated by Frederic Valentin.

✉ Miguel Ángel Moreles
moreles@cimat.mx

Daniel A. Cervantes
dcchivela@ciencias.unam.mx

Pedro González Casanova
casanova@matem.unam.mx

Christian Gout
christian.gout@insa-rouen.fr

[1] Instituto de Matemáticas, UNAM, Ciudad Universitaria, 04510 Mexico, CDMX, Mexico

[2] INSA Rouen, LMI, Av. de lUniversité, BP 08, 76801 St Etienne du Rouvray Cedex, France

[3] CIMAT, Jalisco S/N, 36240 Valenciana, Guanajuato, GTO, Mexico

1 Introduction

The problem of recovering atmospheric wind fields from prescribed horizontal data is of great interest in meteorological applications. In practice, the vertical component is unavailable. Consequently, the measured data are complemented with mass consistency to pose a variational problem for approximation. This approach dates back to Sasaki (1958). Literature on the subject is vast, and a timely review is presented in Ratto et al. (1994).

The numerical approximation of the variational problem requires the solution of Poisson boundary value problems. Numerical approximations of the solutions can be obtained conventionally using the finite element method, finite volume method, finite differences, etc. In these methods, mesh managing is computationally expensive. For the wind field adjustment problem, a case can be made for a mesh-free approach in terms of radial basis functions (RBF). See Pepper et al. (2014) and Cervantes et al. (2013).

In the context of RBF, the problem of wind field recovery has been also considered as a smoothing problem. Mass consistency is introduced by penalizing with the norm of the divergence of the vector field. For the case of polyharmonic splines, Benbourhim and Bouhamidi (2008) developed a smoothing algorithm for a given set of prescribed data in two and three dimensions. A full convergence analysis is provided. These RBF techniques can be traced back to Duchon's works on thin plate splines (Duchon 1977).

The objective here is to build on these methodologies and contribute to two unresolved issues. The wind field adjustment problem is posed on a bounded domain and boundary conditions are to be imposed, for instance the topography of the surface. The smoothing approach considers for approximation a linear combination of polyharmonic splines, and imposing boundary conditions is not straightforward. In the Sasaki's approach, boundary conditions are imposed somewhat heuristically. Also, given that only the first two components of the field are known, an initial guess of the third component is required in this approach. The common practice is unsatisfactory: *since measurements of the vertical velocity component are seldom available, the initial vertical is usually set to zero* (Ratto et al. 1994).

Consequently, in this work the problem is dealt with the data available in practice. Namely, the least squares functional to be introduced only involves the two known components. Minimization is carried out on descent directions; boundary conditions arise naturally and can be imposed on physical grounds. An RBF method is used for approximation. It shall become apparent that our methodology can be complemented with a data preprocessing strategy to deal with realistic, atmospheric wind fields. Finally, a proper abstract setting for analysis and numerics is provided. One motivation is to provide a comprehensive mathematical foundation for wind field adjustment.

This article is organized as follows.

In Sect. 2, the Hilbert function spaces are introduced, and the variational problem is formulated. From basic results form minimization of convex functionals on Hilbert spaces, existence of minima is proven. The construction of the adjusted mass consistent field forms the content of Sect. 3. Also, the Sasaki solution is derived as a particular case. In Sect. 4, we discuss the scheme of the proposed method, and address the boundary conditions for the Poisson problems arising form the line search algorithm and the RBF discretization. Numerical results are presented in Sect. 5; noteworthy is the vortex field in Benbourhim and Bouhamidi. Conclusions and comments on future research close this exposition.

2 Reconstruction of mass consistent vector fields with unknown vertical component

2.1 Problem formulation

Assume that the first two components of a 3D vector field are known at N nonuniform points, namely, $\mathbf{U}_i^0 = (u_1(\mathbf{x}_i), u_2(\mathbf{x}_i)),\ i = 1, 2, \ldots, N$, for $\mathbf{x}_i \in \Omega \subset \mathbb{R}^3$.

Problem Construct a flow field $\mathbf{u}(\mathbf{x}) = (u_1(\mathbf{x}), u_2(\mathbf{x}), u_3(\mathbf{x}))$ in the entire domain Ω, assuming that the set of discrete field values are known and that the approximant satisfies the continuity equation:

$$\nabla \cdot \mathbf{u} = 0.$$

The classical approach is as follows:

1. Initialization. From $\mathbf{U}_i^0,\ i = 1, 2, \ldots, N$, determine an initial field $\mathbf{u}^0(x)$ entirely in Ω.
2. Correction. By means of a minimization procedure, adjust $\mathbf{u}^0$ to a reconstructed field satisfying mass conservation.

Our focus is on (2).

Function spaces
Let $\Omega \subset \mathbb{R}^3$ with boundary Γ. We assume that Ω is a Lipschitz domain. We shall be concerned with n-dimensional vector functions. As customary, we denote

$$\mathbf{L}^2(\Omega) = (L^2(\Omega))^n.$$

Let $\mathbf{E}(\Omega) \equiv E(\Omega)^n$ be the space

$$\mathbf{E}(\Omega) = \{\mathbf{u} \in \mathbf{L}^2(\Omega) : \nabla \cdot \mathbf{u} \in L^2(\Omega)\}.$$

This is a Hilbert space when equipped with the inner product

$$\langle \mathbf{u}, \mathbf{v} \rangle_{\mathbf{E}(\Omega)} = \langle \mathbf{u}, \mathbf{v} \rangle_{\mathbf{L}^2(\Omega)} + \langle \nabla \cdot \mathbf{u}, \nabla \cdot \mathbf{v} \rangle_{L^2(\Omega)}.$$

The subspace of divergence free fields is defined by

$$\mathbf{E}_0(\Omega) = \{\mathbf{h}_1 \in \mathbf{E}(\Omega) : \nabla \cdot \mathbf{h}_1 = 0\}.$$

Let us define the observation operator

$$\mathcal{M} : L(\Omega)^3 \to L(\Omega)^2,$$

by

$$\mathcal{M}(\mathbf{u}) = (u_1, u_2) \equiv \mathbf{U}.$$

It is readily seen that in these L^2 spaces, $\mathcal{M}^*\mathbf{U} = (U_1, U_2, 0)$.
Let $\mathbf{U}^0 \in L(\Omega)^2$ be the given field. Let us define

$$J : \mathbf{E}(\Omega) \to \mathbb{R}$$

by

$$J(\mathbf{u}) = \frac{1}{2}\|\mathcal{M}(\mathbf{u}) - \mathbf{U}^0\|^2_{\mathbf{L}^2(\Omega),S},$$

where

$$\langle \mathbf{U}, \mathbf{V} \rangle_{\mathbf{L}^2(\Omega), S} = \int_\Omega (S\,\mathbf{U}) \cdot \mathbf{V}$$

and S is a symmetric positive definite matrix. For real data, the choice of the matrix S is nontrivial. A simple estimation can be obtained as the inverse of the sample covariance matrix.

We consider the problem:

$$\text{minimize} J(\mathbf{u}) \quad \text{subject to} \quad \nabla \cdot \mathbf{u} = 0.$$

2.2 Existence of minima

In what follows, we shall use freely basic results from minimization of convex functionals on Hilbert spaces. See Zeidler (2013).

It is apparent that J is Gateaux differentiable (G-differentiable). Let $\mathbf{h}_1, \mathbf{k}_1 \in \mathbf{L}^2(\Omega)$; it is readily seen that the first variation of J at $\mathbf{u}$ in the direction $\mathbf{h}_1$ is

$$\delta J(\mathbf{u}; \mathbf{h}_1) = \langle \mathbf{h}_1, \mathcal{M}^* S(\mathcal{M}\mathbf{u} - \mathbf{U}^0) \rangle_{\mathbf{L}^2(\Omega)}, \tag{1}$$

whereas the second variation is given by

$$\delta^2 J(\mathbf{u}; \mathbf{h}_1, \mathbf{k}_1) = \langle \mathbf{h}_1, \mathcal{M}^* S \mathcal{M} \mathbf{k}_1 \rangle_{\mathbf{L}^2(\Omega)}. \tag{2}$$

We obtain the Taylor formula

$$J(\mathbf{v}) = J(\mathbf{u}) + \delta J(\mathbf{u}; \mathbf{v} - \mathbf{u}) + \frac{1}{2} \langle \mathbf{v} - \mathbf{u}, \mathcal{M}^* S \mathcal{M} \mathbf{v} - \mathbf{u} \rangle_{\mathbf{L}^2(\Omega)}. \tag{3}$$

Note that for all $\mathbf{u}, \mathbf{h}_1 \in \mathbf{L}^2(\Omega)$,

$$\delta^2 J(\mathbf{u}; \mathbf{h}_1) \equiv \delta^2 J(\mathbf{u}; \mathbf{h}_1, \mathbf{h}_1) \geq 0.$$

Consequently, J is convex. Equivalently, for $\mathbf{v} \in \mathbf{L}^2(\Omega)$, we have

$$J(\mathbf{v}) \geq J(\mathbf{u}) + \delta J(u; \mathbf{v} - \mathbf{u}).$$

We are led to

Proposition *If F is a bounded, closed and convex subset of $\mathbf{L}^2(\Omega)$, the convex functional*

$$J : \mathbf{L}^2(\Omega) \to \mathbb{R}$$

has a minimum.

We observe that $\mathbf{u}^0 = (U_1^0, U_2^0, 0)$ is a trivial minimum in $\mathbf{L}^2(\Omega)$, not necessarily in $\mathbf{E}_0(\Omega)$. A correction is constructed below.

3 The adjusted field by line search in $\mathbf{E}(\Omega)$

Let us restrict the functional J to $\mathbf{E}(\Omega)$ and assume a given field $\mathbf{u}_c$ and a direction $\mathbf{p}$. We show that there is a unique divergence free field, the *adjusted field*, minimizing J along the line $\mathbf{u}_c + t\mathbf{p}$, $t \in \mathbb{R}$. The choice of the direction $\mathbf{p}$ leads to the solution of a boundary value problem for an elliptic problem. It will become apparent that well-known solutions in the literature are particular cases, of which noteworthy is the Sasaki's solution.

For the computations that follow, the next technical lemma for integration by parts is required.

Lemma 1 *Let* $\Omega \subset \mathbb{R}^d$, $d \geq 2$, *be a bounded Lipschitz domain with boundary* Γ. *Then for all* $\lambda \in H^1(\Omega)$ *and* $\mathbf{h}_1 \in \mathbf{E}(\Omega)$,

$$\int_\Omega \lambda \nabla \cdot \mathbf{h}_1 \, \mathrm{d}x = \int_{\partial\Omega} \lambda \mathbf{h}_1 \cdot \nu \, \mathrm{d}\Gamma - \int_\Omega \nabla\lambda \cdot \mathbf{h}_1 \, \mathrm{d}x, \tag{4}$$

where

$$\int_{\partial\Omega} \lambda \mathbf{h}_1 \cdot \nu \, \mathrm{d}\Gamma$$

is well defined in the sense of the generalized trace with

$$\mathbf{h}_1 \cdot \nu \in H^{-1/2}(\Gamma), \quad \lambda \in H^{1/2}(\Gamma).$$

Proof (Lemma II.1.2.3 in Sohr 2012).

3.1 The adjusted field

Let $f(t)$ be the scalar quadratic function

$$f(t) = J(\mathbf{u}_c + t\mathbf{p}),$$

where $\mathbf{u}_c$ is the base field and $\mathbf{p}$ a descendent direction. By (3), we have

$$f(t) = J(\mathbf{u}_c) + t\langle \mathbf{p}, \mathcal{M}^* S(\mathcal{M}\mathbf{u}_c - \mathbf{U}^0)\rangle_{\mathbf{L}^2(\Omega)} + \frac{t^2}{2}\langle \mathbf{p}, \mathcal{M}^* S \mathcal{M}\mathbf{p}\rangle_{\mathbf{L}^2(\Omega)}. \tag{5}$$

Consequently, for nontrivial $\mathbf{p}$ there exists a unique t_c such that

$$\mathbf{u}_+ = \mathbf{u}_c + t_c\mathbf{p}$$

is the minimizer along the line.

We call $\mathbf{u}_+$ the *adjusted field* for the field $\mathbf{u}_c$ at direction $\mathbf{p}$.

3.2 Incomplete data

Let us consider J restricted to $\mathbf{E}(\Omega)$. To complete the inner product in $\mathbf{E}(\Omega)$, we consider $\lambda \in H^2(\Omega)$ and write

$$\begin{aligned} f(t) = {} & J(\mathbf{u}_c) + t\langle \mathbf{p}, \mathcal{M}^* S(\mathcal{M}\mathbf{u}_c - \mathbf{U}^0) - \nabla\lambda\rangle_{\mathbf{E}(\Omega)} + \frac{t^2}{2}\langle \mathbf{p}, \mathcal{M}^* S\mathcal{M}\mathbf{p}\rangle_{\mathbf{L}^2(\Omega)} \\ & + t(\langle \mathbf{p}, \nabla\lambda\rangle_{\mathbf{L}^2(\Omega)} - \langle \nabla\cdot\mathbf{p}, \nabla\cdot(\mathcal{M}^* S(\mathcal{M}\mathbf{u}_c - \mathbf{U}^0) - \nabla\lambda)\rangle_{\mathbf{L}^2(\Omega)}). \end{aligned} \tag{6}$$

For the multiplier, we require

$$\Delta\lambda = \nabla\cdot(\mathcal{M}^* S(\mathcal{M}\mathbf{u}_c - \mathbf{U}^0)). \tag{7}$$

We seek divergence-free directions, $\nabla\cdot\mathbf{p} = 0$, thus Lemma 1, which implies

$$\langle \mathbf{p}, \nabla\lambda\rangle_{\mathbf{L}^2(\Omega)} = \int_\Gamma \lambda\mathbf{p}\cdot\nu \mathrm{d}\Gamma.$$

If λ and $\mathbf{p}$ are chosen so that

$$\int_\Gamma \lambda\mathbf{p}\cdot\nu \mathrm{d}\Gamma = 0, \tag{8}$$

then (6) becomes

$$f(t) = J(\mathbf{u}_c) + t\langle \mathbf{p}, \mathcal{M}^* S(\mathcal{M}\mathbf{u}_c - \mathbf{U}^0) - \nabla\lambda\rangle_{\mathbf{E}(\Omega)} + \frac{t^2}{2}\langle \mathcal{M}\mathbf{p}, S\mathcal{M}\mathbf{p}\rangle_{\mathbf{L}^2(\Omega)}.$$

Hence, if the first two components of $\mathbf{p}$ form a nontrivial vector, there is a unique minimizer, which yields the adjusted field.

Let $\mathbf{p}$ be the steepest descent direction, namely,

$$\mathbf{p} = -(\mathcal{M}^* S(\mathcal{M}\mathbf{u}_c - \mathbf{U}^0) - \nabla\lambda),$$

and append one of the following boundary conditions to cancel the integral term (8), in $f(t)$,

$$(\mathcal{M}^* S(\mathcal{M}\mathbf{u}_c - \mathbf{U}^0) - \nabla\lambda) \cdot \nu = 0 \quad \text{or} \quad \lambda = 0 \quad \text{for } \lambda \text{ on } \Gamma, \tag{9}$$

then

$$f(t) = J(\mathbf{u}_c) - t\langle \mathbf{p}, \mathbf{p}\rangle_{\mathbf{L}^2(\Omega)} + \frac{t^2}{2}\langle S\mathcal{M}\mathbf{p}, \mathcal{M}\mathbf{p}\rangle_{\mathbf{L}^2(\Omega)}.$$

The adjusted field is given by

$$\mathbf{u}_+ = \mathbf{u}_c - t_c(\mathcal{M}^* S(\mathcal{M}\mathbf{u}_c - \mathbf{U}^0) - \nabla\lambda),$$

where

$$t_c = \frac{\langle \mathbf{p}, \mathbf{p}\rangle_{\mathbf{L}^2(\Omega)}}{\langle S\mathcal{M}\mathbf{p}, \mathcal{M}\mathbf{p}\rangle_{\mathbf{L}^2(\Omega)}}.$$

3.3 The Sasaki's adjusted field

In the classical Sasaki's approach, the functional

$$J(\mathbf{u}) = \int_\Omega [\alpha_1^2(u_1 - u_1^0)^2 + \alpha_2^2(u_2 - u_2^0)^2 + \alpha_3^2(u_3 - u_3^0)^2]\mathrm{d}V$$

is considered for correction. The initial vertical velocity u_3^0 is usually set to zero. The α_is are the so-called Gauss precision moduli.

We address this problem in our general setting. The L^2 space is weighted by S, a 3×3 symmetric positive definite matrix.

Assume that a complete initial field $\mathbf{u}^0 \in (L^2(\Omega))^3$ is given. The corresponding observation operator is

$$\mathcal{I} : \mathbf{L}(\Omega)^3 \to \mathbf{L}(\Omega)^3,$$

given by

$$\mathcal{I}(\mathbf{u}) = \mathbf{u},$$

the identity operator.

In this case we have

$$f(t) = J(\mathbf{u}_c) + t\langle \mathbf{p}, S(\mathbf{u}_c - \mathbf{u}^0)\rangle_{\mathbf{L}^2(\Omega)} + \frac{t^2}{2}\langle \mathbf{p}, S\mathbf{p}\rangle_{\mathbf{L}^2(\Omega)}.$$

Completing the inner product in $\mathbf{E}(\Omega)$ as before,

$$f(t) = J(\mathbf{u}_c) + t\langle \mathbf{p}, S(\mathbf{u}_c - \mathbf{u}^0) - \nabla\lambda\rangle_{\mathbf{L}^2(\Omega)} + \frac{t^2}{2}\langle \mathbf{p}, S\mathbf{p}\rangle_{\mathbf{L}^2(\Omega)} + t\langle \mathbf{p}, \nabla\lambda\rangle_{\mathbf{L}^2(\Omega)} \tag{10}$$

or

$$f(t) = J(\mathbf{u}_c) + t\langle S\mathbf{p}, \mathbf{u}_c - \mathbf{u}^0 - S^{-1}\nabla\lambda\rangle_{\mathbf{E}(\Omega)} + \frac{t^2}{2}\langle S\mathbf{p}, \mathbf{p}\rangle_{\mathbf{L}^2(\Omega)}$$
$$+ t(\langle \mathbf{p}, \nabla\lambda\rangle_{\mathbf{L}^2(\Omega)} - \langle \nabla\cdot(S\mathbf{p}), \nabla\cdot(\mathbf{u}_c - \mathbf{u}^0 - S^{-1}\nabla\lambda)\rangle_{\mathbf{L}^2(\Omega)}). \quad (11)$$

For the multiplier λ we now require

$$\nabla\cdot(S^{-1}\nabla\lambda) = \nabla\cdot(\mathbf{u}_c - \mathbf{u}^0),$$

with boundary conditions

$$(\mathbf{u}_c - \mathbf{u}^0 - S^{-1}\nabla\lambda)\cdot\nu = 0 \quad \text{or} \quad \lambda = 0, \quad \text{for } \lambda \quad \text{on } \Gamma.$$

Letting

$$\mathbf{p} = -(\mathbf{u}_c - \mathbf{u}^0 - S^{-1}\nabla\lambda),$$

be the steepest descent direction, we obtain the adjusted field

$$\mathbf{u}_+ = \mathbf{u}_c - t_c(\mathbf{u}_c - \mathbf{u}^0 - S^{-1}\nabla\lambda).$$

It follows at once that

$$f(t) = J(\mathbf{u}_c) - t\langle S\mathbf{p}, \mathbf{p}\rangle_{\mathbf{L}^2(\Omega)} + \frac{t^2}{2}\langle S\mathbf{p}, \mathbf{p}\rangle_{\mathbf{L}^2(\Omega)},$$

so that

$$t_c = 1.$$

This leads to

$$\mathbf{u}_+ = \mathbf{u}^0 + S^{-1}\nabla\lambda. \quad (12)$$

Hence, if $\mathbf{u}_c = 0$ we obtain the Sasaki's solution.

4 Discretization scheme of the proposed method

Let us describe step by step the implementation and discretization of the adjusted field above.

Assume that $\mathbf{u}_c \in \mathbf{E}_0(\Omega)$ and $\mathbf{U}^0 \in (L^2(\Omega))^2$ are given. For instance, the latter can be obtained by RBF smooothing of the scattered data.

1. Compute the *extended weighted initial residual* $\mathbf{R}_0$, namely

$$\mathbf{R}_0 = \mathcal{M}^* S(\mathcal{M}\mathbf{u}_c - \mathbf{U}^0).$$

2. Introduce appropriate boundary conditions $\mathcal{B}\lambda = g$ on Γ and solve by the RBF method, see below, the elliptic boundary value problem

$$\Delta\lambda = \nabla\cdot\mathbf{R}_0.$$

3. Compute the descent direction

$$\mathbf{p} = -(\mathbf{R}_0 - \nabla\lambda).$$

Derivatives of λ are computed analytically from its RBF expansion.

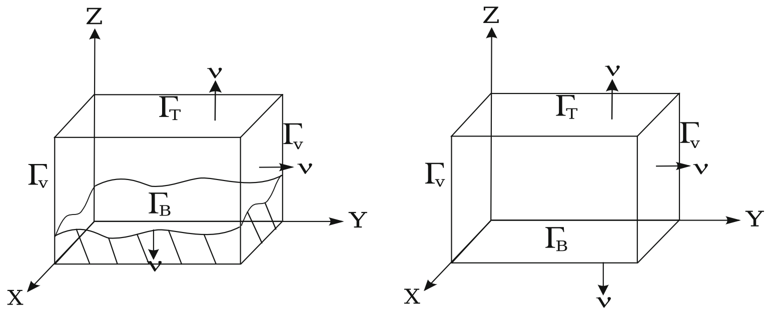

Fig. 1 Bounded domain with and without topography

4. Apply a quadrature rule in the integrals defining the critical step t_c.

$$t_c = \frac{\langle \mathbf{p}, \mathbf{p} \rangle_{\mathbf{L}^2(\Omega)}}{\langle S\mathcal{M}\mathbf{p}, \mathcal{M}\mathbf{p} \rangle_{\mathbf{L}^2(\Omega)}}.$$

5. Compute the adjusted field

$$\mathbf{u}_+ = \mathbf{u}_c - t_c(\mathbf{R}_0 - \nabla\lambda).$$

For wind field recovery a bounded domain is considered as shown in Fig. 1. An irregular bottom boundary models the topography of the terrain. In this context, we prescribe appropriate boundary conditions and introduce the RBF method for the solution of the elliptic problem.

4.1 Boundary conditions

Given an initial field $\mathbf{U}^0$, a correction is through a line search in the direction of a Lagrange multiplier which satisfies the Poisson boundary value problem (PBVP), given by (7) and (9). In the latter, we are led to prescribe $\mathbf{u}_c$ where appropriate, namely:

– *Flow-through* The flux related to the vector field changes due to the mass balance through the boundary Γ. Thus, $\nabla\lambda \neq \mathbf{0}$, implying that one of the components (usually the normal component) of the adjusted vector field is nonzero, but unknown. To fulfill (9), $\lambda = \mathbf{0}$ is applied.
– *No-flow-through* This condition corresponds to the topography region Γ_B. There is no vertical component; hence $\mathbf{u}_c \cdot \nu = 0$.
– *Dirichlet* In cases where the vector field is known on boundary Γ (denoted by $\mathbf{u}_\Gamma$), we set $\mathbf{u}_c \cdot \nu = \mathbf{u}_\Gamma \cdot \nu$. For instance, in vertical borders Γ_V, the available information is the observed field $\mathbf{U}^0$. We require $\mathbf{u}_c \cdot \nu = \mathbf{U}^0 \cdot \nu$.

4.2 RBF asymmetric collocation

The asymmetric collocation method (Kansa 1990) is the most widely used technique for solving PDEs problems. The nodes are divided into the interior and boundary nodes, the ansatz is build on each subset of nodes and it is replaced by the analytic solution in the PDE and its boundary operators. This generates an algebraic system whose solution gives the coefficients of the approximated solution.

In our case, the argument goes as follows. Consider the boundary value problem for λ,

$$\begin{cases} \Delta\lambda = \nabla \cdot \mathbf{R}_0 & \lambda \in \Omega \\ \mathcal{B}\lambda = g & \lambda \in \Gamma. \end{cases} \tag{13}$$

Assuming given a set of N knots $\{\mathbf{x}_i\}_{i=1}^{N} = \{\mathbf{x}_i\}_{i=1}^{N_I} \cup \{\mathbf{x}_i\}_{i=N_I+1}^{N} \subset \Omega \cup \partial\Omega$. Set

$$\hat{\lambda}(\mathbf{x}) := \sum_{i=1}^{N} \alpha_j \phi(\|\mathbf{x} - \mathbf{x}_j\|), \tag{14}$$

where $\|\cdot\|$ is the Euclidean norm. The asymmetric collocation method implies the next lineal system,

$$\begin{pmatrix} \Delta\phi_{11} & \cdots & \Delta\phi_{1N} \\ \vdots & & \vdots \\ \Delta\phi_{N_I 1} & \cdots & \Delta\phi_{N_I N} \\ \mathcal{B}\phi_{N_{I+1}1} & \cdots & \mathcal{B}\phi_{N_{I+1}N} \\ \vdots & & \vdots \\ \mathcal{B}\phi_{N1} & \cdots & \mathcal{B}\phi_{NN} \end{pmatrix} \begin{pmatrix} \alpha_1 \\ \vdots \\ \alpha_{N_I} \\ \alpha_{N_I+1} \\ \vdots \\ \alpha_N \end{pmatrix} = \begin{pmatrix} f(\mathbf{x}_1) \\ \vdots \\ f(\mathbf{x}_{N_I}) \\ g(\mathbf{x}_{N_I+1}) \\ \vdots \\ g(\mathbf{x}_N) \end{pmatrix},$$

where $\phi_{ij} := \phi(\|\mathbf{x}_i - \mathbf{x}_j\|)$ and $f(\mathbf{x}_i) := \nabla \cdot \mathbf{R}_0(\mathbf{x}_i)$.

Remark Let us recall some basics of RBF methods; for further details see Wendland (2005). The expansion in (14) is valid if the function ϕ is a positive definite radial function. For a positive semidefinite radial function, a polynomial correction is required. We limit ourselves to the former. The collocation method leads to a linear system, say $G\beta = b$. G is known as the Gram's matrix. Albeit its simplicity and proven performance on numerical solution of partial differential equations (Sarra 2008), invertibility of the Gram's matrix is an open problem.

5 Numerical examples

In the following examples, we illustrate the application of the line search method above. We analyse its performance when recovering the unknown vertical component of zero divergence fields. In all examples, we use Dirichlet data.

For the numerical approximation, we shall use the ansatz (14), using inverse multiquadrics,

$$\phi(r) = \frac{1}{\sqrt{(1 + (rc)^2)}},$$

where c is the shape parameter, whose value is related to the spectral convergence of the approximation (Fornberg and Flyer 2005). Because of its highly satisfactory performance, inverse multiquadrics is one of the preferred choices for RBF approximation.

We complement the scheme in Sect. 4 with the specifics of the numerical examples that follow.

1. The shape parameter is chosen to have an accurate numerical solution of the Poisson problem. From our extensive numerical experiments, we found that computation of the adjusted field gives excellent results in all examples for $c = 0.01$ or $c = 0.001$.

Table 1 Example 5.1. Vector field approximation ($\mathbf{u}_+$) of $\mathbf{u}(x, y) = (x, y, -2z)$ on $(-2, 2) \times (-2, 2) \times (0, 2)$ using a set of equidistant centers

N	c	$\kappa(G)$	$\nabla \cdot u_+$	$\|u_+ - \mathbf{u}\|_2/\|\mathbf{u}\|_2$
27	0.001	2.252627e+18	4.679924e−05	2.707875e−05
125	0.001	5.801561e+19	1.088109e−06	5.342928e−06
512	0.001	1.195701e+20	7.873625e−08	6.961732e−08

2. We assume no previous knowledge of the field in the open set Ω. So, we make the trivial choice $\mathbf{u}_c = \mathbf{0}$. This implies that the initial field $\mathbf{u}^0$ is the data $\mathbf{U}^0$ appended with zero third component.
3. The choice of the weighing matrix S presumes some knowledge on the statistics of the problem. We are content in this work with synthetic deterministic examples and set S as the identity matrix.
4. We are led to solve $\Delta\lambda = -\nabla \cdot \mathbf{u}^0$. For illustration we consider only Dirichlet boundary conditions. We consider the same uniform mesh for data and numerical solution of the boundary value problem.
5. The critical time step is $t_c = 1$, which yields the Sasaki's adjusted field

$$\mathbf{u}_+ = \mathbf{u}^0 + \nabla\lambda.$$

Example 1 Let us consider an extension of the 2D field in Cervantes et al. (2013), namely $\mathbf{u}(x, y, z) = (x, y, -2z)$ on the domains $\Omega_1 = (-2, 2) \times (-2, 2) \times (0, 2)$ and $\Omega_2 = (-2, 2) \times (-2, 2) \times (-2, 2)$ (which are shown on the left side of Fig. 2 in a stream ribbon style). Here, $\mathbf{u}^0(x, y, z) = (x, y, 0)$, so that in Ω_1 (domain with topography) we impose a no-flow-through boundary condition on Γ_B, while in Ω_2 a Dirichlet boundary condition is used on Γ_B (see Fig. 1).

The results are shown in Table 1 and in the right hand side of Fig. 2. In Table 1, only the results for Ω_1 are displayed. The corresponding results for Ω_2 are nearly equivalent. The relative error and the approximated divergence decrease as the number of centers increases. As expected, the condition number of Gram matrix increases. This is a well-known and classic behavior of the schemes based on radial basis functions, the so-called *Schaback uncertainty principle* (Schaback 1995).

Example 2 In this example, we approximate the (nontrivial) vortex-type vector field in Benbourhim and Bouhamidi (2008). It is shown on the left side of Fig. 3 in a stream ribbon style and is given by

$$\mathbf{u}(x, y, z) = \left(2ye^{-\frac{(x^2+y^2+z^2)}{49}}, -2xe^{-\frac{(x^2+y^2+z^2)}{49}}, 1\right),$$

with $\Omega = (-7, 7) \times (-7, 7) \times (-7, 7)$. The initial field is taken as

$$\mathbf{u}^0(x, y, z) = \left(2ye^{-\frac{(x^2+y^2+z^2)}{49}}, -2xe^{-\frac{(x^2+y^2+z^2)}{49}}, 0\right).$$

In this case, we do not consider the topography and assume that the vector field in the upper and lower regions is known. That is, Dirichlet boundary conditions for Γ_T and Γ_B are considered. The results are shown in Table 2 and in the right hand side of Fig. 3.

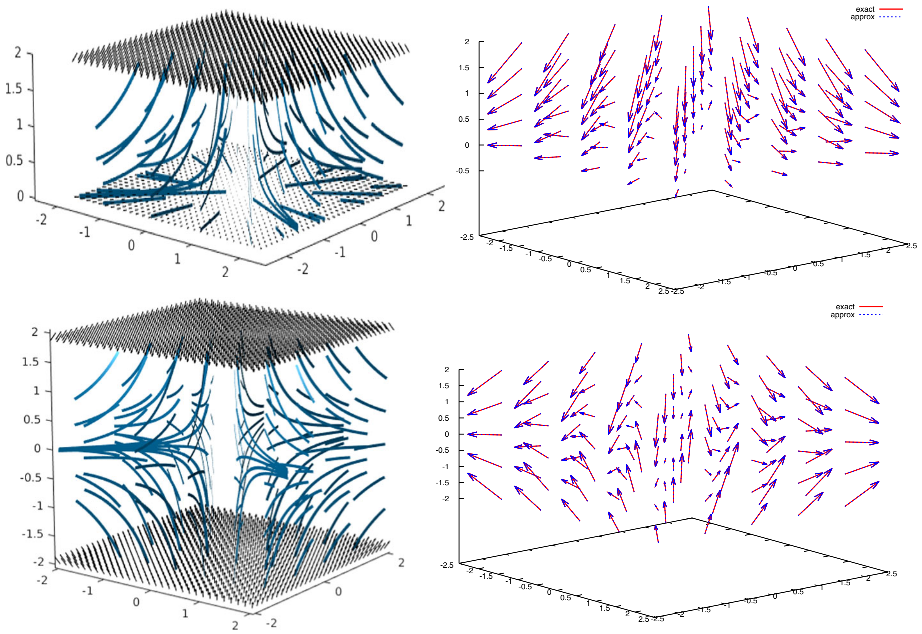

Fig. 2 Example 5.1. *Left* vector field $\mathbf{u}(x, y, z) = (x, y, -2z)$ on $(-2, 2) \times (-2, 2) \times (0, 2)$ and $(-2, 2) \times (-2, 2) \times (-2, 2)$. *Right* vector field approximation taking $\mathbf{u}^0 = (x, y, 0)$, the *solid arrows* and *dotted arrows* represent, respectively, the exact and the approximated vector field

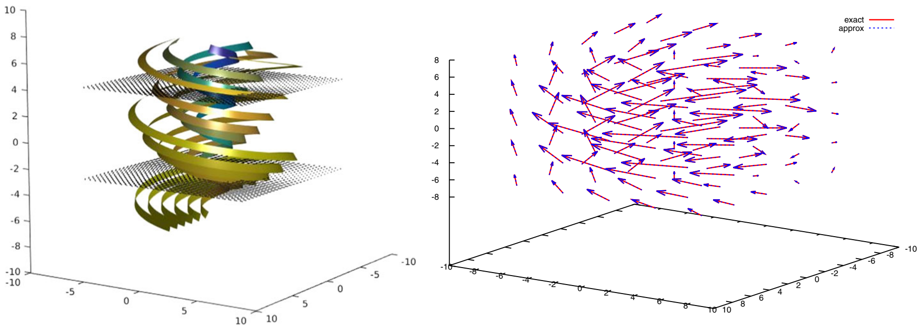

Fig. 3 Example 5.2. *Left* vector field $\mathbf{u}(x, y, z) = (2ye^{\frac{-(x^2+y^2+z^2)}{49}}, -2xe^{\frac{-(x^2+y^2+z^2)}{49}}, 1)$ on $(-7, 7) \times (-7, 7) \times (-7, 7)$. *Right* vector field approximation taking taking $\mathbf{u}^0(x, y, z) = (2ye^{-\frac{(x^2+y^2+z^2)}{49}}, -2xe^{-\frac{(x^2+y^2+z^2)}{49}}, 0)$. The *solid arrows* and *dotted arrows* represent, respectively, exact and approximated vector field

Example 3 In this last example, we consider a variant of Example 5.2 to have a topography in the xy plane. Consequently, the no-flow-through boundary condition is imposed on Γ_B.

The vector field is given by

$$\mathbf{u}(x, y, z) = \left(2ye^{-\frac{(x^2+y^2+z^2)}{49}} - \varepsilon\frac{xz}{2}, -2xe^{-\frac{(x^2+y^2+z^2)}{49}} - \varepsilon\frac{yz}{2}, \varepsilon\frac{z^2}{2}\right),$$

Table 2 Example 5.2. Vector field approximation ($\mathbf{u}_+$) of $(2ye^{-\frac{(x^2+y^2+z^2)}{49}}, -2xe^{-\frac{(x^2+y^2+z^2)}{49}}, 1)$ on $(-7,7)\times(-7,7)\times(-7,7)$ using a set of equidistant centers

N	c	$\kappa(G)$	$\nabla\cdot u_+$	$\Vert u_+ - \mathbf{u}\Vert_2/\Vert\mathbf{u}\Vert_2$
27	0.01	6.468932e+09	−5.553522e−06	4.879887e−03
125	0.01	5.736571e+18	−6.975779e−03	2.968737e−05
512	0.01	1.057278e+20	−5.411860e−03	1.226800e−07

Table 3 Example 5.3. Vector field approximation ($\mathbf{u}_+$) of $\mathbf{u}(x,y) = (2ye^{-\frac{(x^2+y^2+z^2)}{49}} - \varepsilon\frac{xz}{2}, -2xe^{-\frac{(x^2+y^2+z^2)}{49}} - \varepsilon\frac{yz}{2}, \varepsilon\frac{z^2}{2})$ on $(-7,7)\times(-7,7)\times(0,7)$ using a set of equidistant centers

N	c	ϵ	$\kappa(G)$	$\nabla\cdot u_+$	$\Vert u_+ - u\Vert_2/\Vert u\Vert_2$
27	0.01	0.1	1.508177e+13	2.633422e−03	1.463895e−01
125	0.01	0.1	2.632883e+21	4.063153e−03	4.732374e−04
512	0.01	0.1	8.866826e+21	1.365358e−02	5.872183e−05

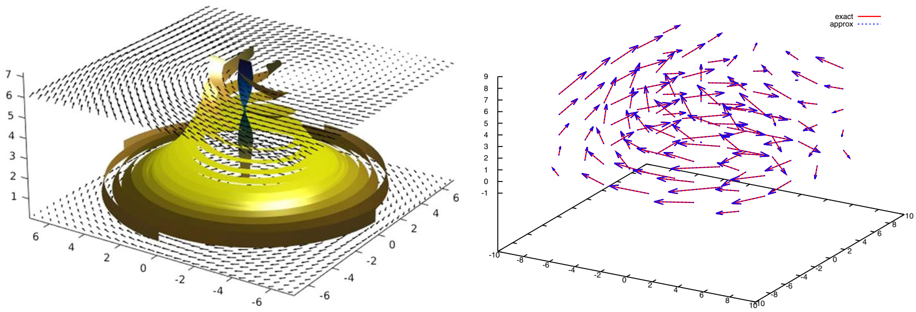

Fig. 4 Example 5.3. *Left* vector field $\mathbf{u}(x,y,z) = (2ye^{\frac{-(x^2+y^2+z^2)}{49}} - \varepsilon\frac{xz}{2}, -2xe^{\frac{-(x^2+y^2+z^2)}{49}} - \varepsilon\frac{xz}{2}, \varepsilon\frac{z^2}{2})$ on $(-7,7)\times(-7,7)\times(0,7)$, for $\varepsilon = 0.1$. *Right* vector field approximation, taking $\mathbf{u}^0(x,y,z) = (2ye^{-\frac{(x^2+y^2+z^2)}{49}} - \varepsilon\frac{xz}{2}, -2xe^{-\frac{(x^2+y^2+z^2)}{49}} - \varepsilon\frac{yz}{2}, 0)$. The *solid arrows* and *dotted arrows* represent, respectively, the exact and approximated vector field

with $\Omega = (-7,7)\times(-7,7)\times(0,7)$ and $\varepsilon > 0 \in \mathbb{R}^+$. As before, the initial field is

$$\mathbf{u}^0(x,y,z) = \left(2ye^{-\frac{(x^2+y^2+z^2)}{49}} - \varepsilon\frac{xz}{2}, -2xe^{-\frac{(x^2+y^2+z^2)}{49}} - \varepsilon\frac{yz}{2}, 0\right).$$

In the left hand side of Fig. 4, we show this vector filed for $\varepsilon = 0.1$ in a stream ribbon style. The corresponding results are shown in Table 3 and in the right hand side of Fig. 4.

Some remarks are in order.

1. The numerical solution of Poisson problems with RBF methods is well documented. All variants have been tried in the literature, such as random placement of the nodes and global and local RBF approaches. Some of the authors in this work have contributed in these directions. In Cervantes et al. (2013), an alternative is proposed to use a local Hermite interpolation method (LHI), which can deal with a considerably larger amount of data. Therein, it is proved that under certain assumptions, the LHI technique can be as

good as the global collocation method. A more recent work illustrating a local approach in the context of wind fields is Pepper and Waters (2016). In the numerical examples above, a global approach with uniform placement of the nodes sufficed. The resulting linear system is solved using an SVD decomposition technique. The full adjustment field method was implemented in MATLAB in an Intel core2 quad CPU 2.50 GHz. The code is available upon request.

2. In the numerical examples, the fields are recovered in the full 3D domain. As shown in the tables, a uniform mesh of 27 nodes yields satisfactory results, with 125 nodes the results are excellent. Noteworthy are the vortex fields in Examples 2 and 3. We are hopeful that with a well-known RBF machinery, a nonuniform mesh with similar resolution will suffice in more realistic examples.
3. An issue of the global RBF approach is the increase of the condition number of the Gram matrix with the number of nodes. Also, the choice of the shape parameter can be challenging. Literature on dealing with these two problems is vast; for instance see Gonzlez-Casanova et al. (2009). Therein, a node and shape parameter adaptive, domain decomposition method is proposed to address these issues for solving real-life problems.
4. Our method starts with a 3D initial field $\mathbf{u}^0(x)$, obtained from the horizontal scattered data field $\mathbf{U}_i^0,\ i = 1, 2, \ldots, N$. It is apparent that the data field need not be horizontal. The construction of the initial field is open to discussion, for instance one way to obtain vertical velocity, at least as a rough estimate, is to solve the continuity equation for the unknown value.

6 Conclusion

In this article, we have introduced a mass consistent variational approach to approximate 3D vector fields from a set of prescribed scattered data values, whose vertical component is unknown. This problem is of great interest for meteorological applications and has been treated in the literature by several authors; see Ratto et al. (1994), for a recent review.

More precisely, a first contribution of this article is our approach, based on the adjoint method; let us build the adjusted field, as the unique solution along an appropriately chosen descent direction. A full analysis of the existence and uniqueness of the solution is proved within the proper Hilbertian setting. Boundary conditions for the adjoint equations arise naturally from the variational formulation in such a way that it is possible to build them according to the physical properties of the field. This point generalizes Sasaki's pioneer approach (Sasaki 1958), which imposes in an heuristic way particular boundary conditions. We prove in fact that Sasaki's method is a particular case of our approach.

Several works, which use classic techniques, like finite elements or finite differences, have appeared in the literature, to solve this problem (see Ratto et al. 1994).

To avoid the computational expansive 3D mesh generation, some radial basis function (RBF) methods have been formulated; see Pepper et al. (2014) and Cervantes et al. (2013).

We recall the work of Benbourhim and Bouhamidi (2008), in which a smoothing algorithm was developed for a given set of physically constrained prescribed data of vector fields in two and three dimensions. Although this is an important method, no boundary conditions can be imposed by this approach in an open bounded set in two or three dimensions.

In our work, a radial mesh-free asymmetric collocation technique is used to discretize the adjoint equations in an open bounded domain. Inverse multiquadric kernels are used, thus providing exponential rate of convergence. Numerical experiments were designed to prove different boundary conditions, namely, when the field is tangential to the terrain and when no terrain is considered. In all cases, the numerical errors and the approximated value of the divergence are excellent for a small number of data.

Several points remain unsolved within the scope of this work. Among them, we mention its possible generalization to approximate vector fields having different physical properties, like zero rotational or elasticity constrains. Also, to approximate real-life data, this method could be restated as a smoothing approximant. Further work is in progress in these directions.

Acknowledgements The authors would like to acknowledge ECOS-NORD project number 000000000263116/M15M01 for financial support during this research. C. Gout thanks the M2NUM project which is co-financed by the European Union with the European Regional Development Fund (ERDF, HN0002137) and by the Normandie Regional Council. Funding was provided by PAPIIT UNAM (Grant No. IN102116). The authors thank the anonymous referees for their very constructive comments and suggestions, leading to a much improved manuscript.

References

Benbourhim M-N, Bouhamidi A (2008) Pseudo-polyharmonic vectorial approximation for div-curl and elastic semi-norms. Numerische Mathematik 109(3):333–364

Cervantes DA et al (2013) Vector field approximation using radial basis functions. J Comput Appl Math 240:163–173

Duchon J (1977) Splines minimizing rotation-invariant semi-norms in Sobolev spaces. Constructive theory of functions of several variables. Springer, Berlin

Fornberg B, Flyer N (2005) Accuracy of radial basis function interpolation and derivative approximations on 1-D infinite grids. Adv Comput Math 23(1–2):5–20

Gonzlez-Casanova P, Muoz-Gmez JA, Rodrguez-Gmez G (2009) Node adaptive domain decomposition method by radial basis functions. Numer Methods Partial Differ Equ 25(6):1482–1501

Kansa EJ (1990) Multiquadrics—a scattered data approximation scheme with applications to computational fluid-dynamics—II solutions to parabolic, hyperbolic and elliptic partial differential equations. Comput Math Appl 19(8):147–161

Pepper DW, Rasmussen C, Fyda D (2014) A meshless method using global radial basis functions for creating 3-D wind fields from sparse meteorological data. Comput Assist Methods Eng Sci 21(3–4):233–243

Pepper DW, Waters J (2016) A local meshless method for approximating 3D wind fields. J Appl Meteorol Climatol 55(1):163–172

Ratto CF et al (1994) Mass-consistent models for wind fields over complex terrain: the state of the art. Environ Softw 9(4):247–268

Sarra A (2008) A numerical study of the accuracy and stability of symmetric and asymmetric RBF collocation methods for hyperbolic PDEs. Numer Methods Partial Differ Equ 24(2) 670–686

Sasaki Y (1958) An objective analysis based on the variational method. J Meteorol Soc Jpn Ser II 36(3):77–88

Schaback R (1995) Error estimates and condition numbers for radial basis function interpolation. Adv Comput Math 3(3):251–264

Sohr H (2012) The Navier–Stokes equations: an elementary functional analytic approach. Springer, Basel

Wendland H (2005) Scattered data approximation. Cambridge University Press, Cambridge

Zeidler E (2013) Nonlinear functional analysis and its applications: III: variational methods and optimization. Springer-Verlag, New York